

Labeling and biodistribution of ^{99m}Tc -7-bromo-1,4-dihydro-4-oxo-quinolin-3-carboxylic acid complex

Reem I. Al-wabli · M. A. Motaleb · Adnan A. Kadi ·
Khalid A. Al-rashood · Wafaa A. Zaghary

Received: 31 May 2011 / Published online: 16 June 2011
© Akadémiai Kiadó, Budapest, Hungary 2011

Abstract 7-Bromo-1,4-dihydro-4-oxo-quinolin-3-carboxylic acid (BDOQCA), was synthesized with a yield of 93% and well characterized. The obtained compound was investigated to label with one of the most important radioactive isotopes (technetium-99m). Effect of BDOQCA concentration, stannous chloride dihydrates ($\text{SnCl}_2 \cdot 2\text{H}_2\text{O}$) concentration, pH and reaction time on the percent labeling yield of ^{99m}Tc -BDOQCA complex was studied in details. ^{99m}Tc -BDOQCA complex was obtained at a maximum yield of 97.3% by mixing 2.5 mg of BDOQCA with 25 μg $\text{SnCl}_2 \cdot 2\text{H}_2\text{O}$ at pH 6 and 30 min reaction time and the formed complex was stable for a time up to 8 h with a maximum yield of 97.3%. Biodistribution studies in mice were carried out using experimentally induced infection in the left thigh using *E. coli*. Both thighs of the mice were dissected and counted to evaluate the ratio of bacterial infected thigh/contralateral thigh. Higher uptake in the infected thigh was observed after 2 h of IV administration of ^{99m}Tc -BDOQCA complex ($T/NT = 7.6 \pm 0.6\%$) than that of the commercially available ^{99m}Tc -ciprofloxacin complex ($T/NT = 3.8 \pm 1\%$). The in vitro binding and biodistribution of ^{99m}Tc -BDOQCA complex in the septic and aseptic inflammation bearing mice showed that, ^{99m}Tc -BDOQCA complex is a promising agent for infection imaging and can differentiate between infected and inflamed muscle.

Keywords Quinolin · ^{99m}Tc · Infection · Inflammation · Diagnosis

Introduction

Many techniques are available for diagnosis of infection and inflammation. These techniques are X-ray, ultrasonography (US), computed tomography (CT) and magnetic resonance imaging (MRI). But it is well known that these are not the best of techniques for the imaging of infection at early stages [1]. The early detection of the infectious focus by radionuclide imaging helps both patient and medical operators and reduces the time and cost of treatment. A number of infection imaging radiotracer were reported including ^{67}Ga -citrate [2, 3], ^{99m}Tc or ^{111}In -labelled leukocytes [4], ^{99m}Tc -nano-colloid [5], ^{99m}Tc or ^{111}In labelled HIG (human polyclonal immunoglobulin) [6, 7] and ^{99m}Tc -ubiquitin 29-4 [8–10]. However, none of the above radiotracer is capable of differentiate in a clinically useful manner between septic and aseptic inflammation [11].

^{99m}Tc labelled ciprofloxacin (fluoroquinolone antibiotic) has been proposed for infection imaging because of its simple binding procedure, immovability and fitting scintigraphic results. ^{99m}Tc -ciprofloxacin is not the best radiotracer for infection imaging because it has many disadvantages related to radiochemical purity and stability [12–15]. The previous reported data about specificity of ^{99m}Tc -ciprofloxacin kit is contradictory [13, 16–22]. Other fluoroquinolone derivatives such as sparfloxacin [23], enrofloxacin, levofloxacin [24], pefloxacin [25], lomefloxacin [16], difloxacin [26], moxifloxacin [27], sitafloxacin [28], rifampicin [29] and norfloxacin [30] are labelled with ^{99m}Tc to be used for infection imaging and to differentiate

R. I. Al-wabli · A. A. Kadi · K. A. Al-rashood ·
W. A. Zaghary (✉)
Department of Pharmaceutical Chemistry, College of Pharmacy,
King Saud University, Riyadh 11495, Saudi Arabia
e-mail: wzaghary@ksu.edu.sa

M. A. Motaleb
Labeled Compound Department, Hot Labs Center,
Atomic Energy Authority, Cairo 13759, Egypt

between septic and aseptic inflammation. Most of the above ^{99m}Tc -fluoroquinolone can not distinguish infection from sterile inflammation. In this study, a new quinolone derivative (7-bromo-1,4-dihydro-4-oxo-quinolin-3-carboxylic acid) was synthesized, well characterized and it is labelling with ^{99m}Tc was investigated. Factors affecting the labeling yield of ^{99m}Tc -BDOQCA complex and biological distribution in inflammation bearing animals were studied in detail.

Experimental

Melting points were determined on Mettler FP 80 melting point apparatus and are uncorrected. Infrared (IR) spectra were recorded on Perkin Elmer FT-IR Spectrum BX Spectrometer at Cm^{-1} scale using KBr discs. $^1\text{H-NMR}$ and $^{13}\text{C-NMR}$ were carried out on Bruker AC 500 MHz and JEOL 300 MHz Spectrometer using TMS as internal stander and chemical shift values were recorded in ppm on δ scale. The $^1\text{HNMR}$ data were represented as follow: chemical shifts, multiplicity (s. single, d. doublet, t. triplet, q. quartet, b. broad) and number of protons. $^{13}\text{CNMR}$ data were represented as chemical shifts and type of carbon. EI mass spectra were determined on LC/MS/MS, 3200QTRAP, AB Applied Biosystems. MDS SCIEX, Cairo, Egypt. Thin layer chromatography was performed on precoated (0.75 mm) silica gel GF₂₅₄ plates (E. Merck, Germany). Visualization was performed by illumination with UV light source (254 nm). BDOQCA was prepared using the modification of previously published procedure [31–35] as described below (Fig. 1).

Synthesis of 7-bromo-3-carbethoxy-1,4-dihydro-4-oxo-quinoline (3)

Mixture of m-bromoaniline (1.7 g, 0.01 mol) and diethyl ethoxymethylene malonate (2.6 g, 0.01 mol) in absolute ethanol (10 ml) was refluxed for 6 h and left over night. The

formed anilide was added to boiling phenyl ether ($\text{Ph}_2\text{O} \approx 200$ ml) with stirring and the mixture was refluxed for 90 min and cooled to room temperature. The resulting 3-carbethoxy-4-hydroxy-7-bromoquinoline was filtered, washed several times with a 2:1 mixture of ethyl acetate and petroleum ether and recrystallized from 70% ethanol to afford 2.1 g (71%). mp > 250 IR (KBr): ν (cm^{-1}) 3447.80, 3085.42, 2924, 2853.02, 1773.82, 1700.11, 1654.32, 1193.79; $^1\text{H NMR}$ (CDCl_3): δ 1.51 (t, 3H, $-\text{CH}_2\text{CH}_3$), 4.65 (q, 2H, CH_2CH_3), 8.03 (d, $J = 10$ Hz, 1H, H_{ar}), 8.42 (s, 1H, H_{ar}), 8.45–8.47 (d, $J = 10$ Hz, 1H, H_{ar}), 9.37 (s, 1H, $\text{N-CH} = \text{C}$), 14.5 (b, 1H, $-\text{NH}$); $^{13}\text{C NMR}$ (CDCl_3): δ 13.47 ($-\text{CH}_2\text{CH}_3$), 65.06 (CH_2CH_3), 105.06–146.49 (8 C_{ar}), 167.63 ($-\text{CO}-$), 174.25 ($-\text{COO}-$); MS m/z (%): 298 ($\text{M}^+ + 2$), 252 (100); Anal. ($\text{C}_{12}\text{H}_{10}\text{BrNO}_3$) C, H, N.

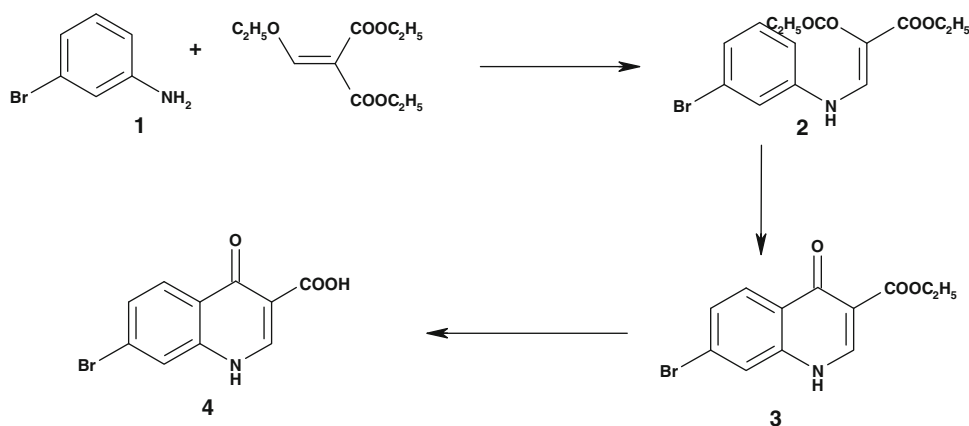
Synthesis of 7-bromo-1,4-dihydro-4-oxo-quinolin-3-carboxylic acid (BDOQCA)

A solution of 3-carbethoxy-4-hydroxy-7-bromoquinoline (1 g) in glacial acetic acid (10 ml), water (10 ml) and hydrochloric acid (10 ml) was heated on steam bath for 8 h. After cooling the solution was diluted with water and filtered, the precipitate was recrystallized from ethanol to afford 0.86 g (93%). mp > 250 IR (KBr): ν (cm^{-1}) 3481–2363, 3068, 1773.68, 1733.98, 1618, 1222; $^1\text{H NMR}$ (CDCl_3): δ 8.07–8.09 (d, $J = 7.5$ Hz, 1H, H_{ar}), 8.35 (s, 1H, H_{ar}), 8.47–8.49 (d, $J = 10$ Hz, 1H, H_{ar}), 9.3 (s, 1H, $\text{N-CH} = \text{C}$), 13.6 (b, 1H, $-\text{OH}$); $^{13}\text{C NMR}$ (CDCl_3): δ 104.06 (C_3), 110.9 (C_8), 113.2–115.5 ($\text{C}_{4,7}$), 117.7–118.8 (C_6), 126.2–129.7 (C_7), 134.2 9 C_5), 140.03 ($\text{C}_{8,9}$), 146.8 (C_2), 169.7 ($-\text{COOH}$), 174.25 (C_4); MS m/z (%): 268 (M^+ , 100), 270 ($\text{M}^+ + 2$, 98); Anal. ($\text{C}_{10}\text{H}_6\text{BrNO}_3$) C, H, N.

Chemicals

All other chemicals were purchased from Merck and they were reactive grade. In all cases, the water used is deoxygenated bidistilled water.

Fig. 1 Reaction scheme for the synthesis of BDOQCA



Labeling of BDOQCA by ^{99m}Tc

Labeling procedure: BDOQCA 0.5–3 mg (with a 0.5 mg increment in each vial) were taken separately in nitrogen filled vials with 5–35 μg of $\text{SnCl}_2 \cdot 2\text{H}_2\text{O}$ with a 5 μg increment in each vial). After gently swirling, 400 MBq of $\text{Na}^{99m}\text{TcO}_4^-$ was added through sterilized syringes to the above preparations. The pH of the preparations was kept from 3.0 to 9.0 (with a 1 increment in each vial) followed by incubation at room temperature and filtration through Millipore filter before investigation.

Analysis

For each labeling experiment, two drops of the reaction product were spotted on two 'Whatman no. 1' ascending chromatographic paper strips (each of $10 \times 1.5 \text{ cm}^2$). One strip was developed with acetone and other strip was developed with ethanol: water: ammonium hydroxide mixture (2:5:1). After complete development, the two radiochromatograms were dried, cut into 0.5 cm pieces and separately counted using the NaI(Tl) scintillation counter to determine the ratio of the hydrolyzed ^{99m}Tc , free $^{99m}\text{TcO}_4^-$ and ^{99m}Tc -complex. It was further confirmed by a Shimadzu HPLC system, which consists of pumps LC-9A, Rheodyne injector and UV spectrophotometer detector (SPD-6A) operated at a wavelength of 320 nm. Chromatographic analysis was performed by injection of 10 μl from the reaction mixture of ^{99m}Tc -quinolon into a reversed-phase column (Lichrosorb RP18, 4 mm \times 250 mm; 5 μm). The column was eluted with 10% ethanol in 0.2 M phosphate buffer pH 7.2 and the flow rate was adjusted to 0.5 ml/min. Then fractions of 0.5 mL were collected separately using a fraction collector up to 20 mL and counted in a well-type γ -scintillation counter.

Stability of ^{99m}Tc -BDOQCA in serum

Stability of ^{99m}Tc -BDOQCA was studied in vitro by mixing 1.8 mL of normal serum and 0.2 mL of ^{99m}Tc -complex and incubated at 37 $^\circ\text{C}$ for 24 h. Exactly 0.2 mL aliquots were withdrawn during the incubation at different time intervals up to 24 h and subjected to ITLC for determination the percent of ^{99m}Tc -complex, reduced hydrolyzed technetium and free pertechnetate.

In vitro binding with *Escherichia coli*

In vitro binding behaviour of the ^{99m}Tc -BDOQCA complexes was investigated using the reported method [36]. Briefly, 10 MBq of the ^{99m}Tc -BDOQCA complex in 0.1 mL of sodium phosphate buffer (Na-PB) was transferred to a clean and sterilized test tube. Thereafter, 0.8 mL

of 50% (v/v) 0.01 M acetic acid in a Na-PB containing approximately 1×10^8 colony forming units (CFU) of *E. coli* were added. The mixture was then incubated at 4 $^\circ\text{C}$ for 1 h. The mixture after 1 h was centrifuged for 5 min at 2000 rpm. The bacterial pellets were resuspended after the removal of supernatant in 1 mL Na-PB and recentrifuged. The *E. coli* pellets after removal of the supernatant analyzed for % activity using well counter.

Induction of infectious foci

A single clinical isolation of *E. coli* from biological samples was used to produce focal infection. Individual colonies were diluted in order to obtain turbid suspension. Groups of three mice were intramuscularly injected with 200 μL of the suspension in the left lateral thigh muscle [37, 38]. Then, the mice were left for 24 h to get a gross swelling in the infected thigh.

Induction of non-infected inflammation

Sterile inflammation was induced by injecting 200 μL of turpentine oil [39]. Sterilized by autoclaving at 121 $^\circ\text{C}$ for 20 min, intramuscularly in the left lateral thigh muscle of the mice. Two days later, swelling appeared.

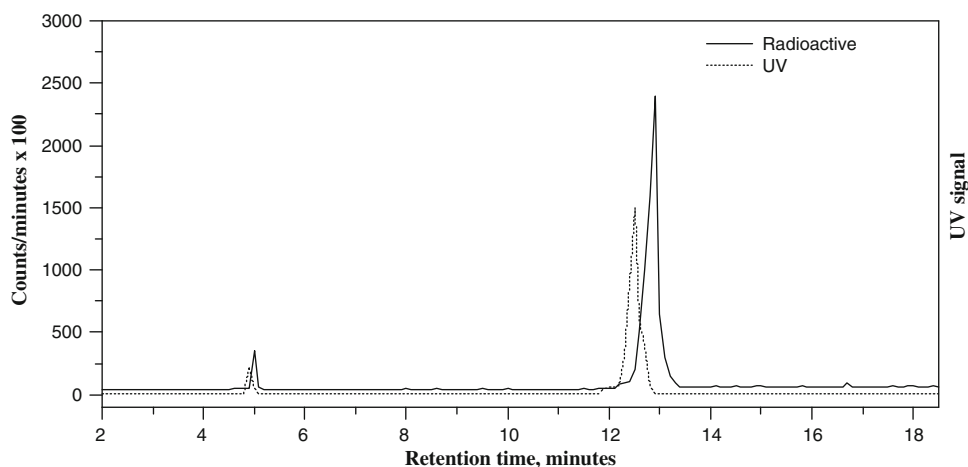
Induction of heat killed *E. coli* non-infected inflammation

Sterile inflammation was induced by injecting 200 μL of heat killed *E. coli*, sterilized by autoclaving at 121 $^\circ\text{C}$ for 20 min, intramuscularly in the left lateral thigh muscle of the mice. Two days later, swelling appeared.

The study was approved by the animal ethics committee, Labeled Compound Department, and was in accordance with the guidelines set out by the Egyptian Atomic Energy Authority.

The animals were intravenously injected with 100 μL (100–150 MBq) ^{99m}Tc -BDOQCA via the tail vein and kept alive in metabolic cage for different intervals of time under normal conditions. The mice were sacrificed at 2, 4 and 24-hour post-injection. Samples of fresh blood, bone and muscle were collected in pre-weighed vials and counted. The different organs were removed, counted and compared to a standard solution of the labeled BDOQCA. The average percent values of the administered dose/organ were calculated. Blood, bone and muscles were assumed to be 7, 10 and 40%, respectively, of the total body weight [40]. Corrections were made for background radiation and physical decay during experiment. Both target and non-target thighs were dissected and counted. Differences in the data were evaluated with the Student's *t* test. Results for

Fig. 2 HPLC chromatogram of ^{99m}Tc -BDOQCA



P using the 2-tailed test are reported and all the results are given as mean \pm SEM. The level of significance was set at $P < 0.05$.

Results and discussion

Like other quinolones, BDOQCA has only one possibility to form complex between ^{99m}Tc and donating atoms where the chelation was formed between ^{99m}Tc and two molecules of BDOQCA each one share with two donor oxygen atoms (one of carbonyl oxygen and other of carboxyl oxygen) [14, 24, 43].

Radiochemical purity and stability of ^{99m}Tc -BDOQCA complex were assessed by thin layer chromatographic method and reversed phase high performance liquid chromatography (HPLC). In thin layer chromatography using acetone as the solvent, free $^{99m}\text{TcO}_4^-$ moved with the solvent front ($R_f = 1$), while ^{99m}Tc -BDOQCA and reduced hydrolyzed technetium remained at the point of spotting. Reduced hydrolyzed technetium was determined by using ethanol: water: ammonium hydroxide mixture (2:5:1) as the mobile phase, where reduced hydrolyzed technetium remains at the point of spotting ($R_f = 0$) while other species migrate with the solvent front ($R_f = 1$). The radiochemical purity was determined by subtracting the sum of the percent of colloid and free pertechnetate from 100%.

An HPLC radiochromatogram was presented in Fig. 2 and showed two peaks, one at fraction No.5, which corresponds to $^{99m}\text{TcO}_4^-$, while the second peak was collected at fraction No.12.9 for ^{99m}Tc -BDOQCA which was found to coincide with the UV signal.

Effect of substrate concentration

Figure 3 shows that, the radiochemical yield of ^{99m}Tc -BDOQCA complex increased from 38.4 ± 0.76 to

$93.7 \pm 1.87\%$ by increasing the amounts of BDOQCA from 0.5 to 2.5 mg and the main impurities was colloid ($51 \pm 2.25\%$ at 0.5 mg BDOQCA). This low labeling yield was due to the substrate concentrations being insufficient to form complex with all of the reduced technetium so, the remained reduced ^{99m}Tc were converted to colloid. By increasing the substrate concentration over the optimum values (2.5 mg), the labeling yield was slightly decreased which reach to $93 \pm 1.86\%$ at 3 mg BDOQCA.

Effect of $\text{SnCl}_2 \cdot 2\text{H}_2\text{O}$ concentration

As shown in Fig. 4, $25 \mu\text{g}$ $\text{SnCl}_2 \cdot 2\text{H}_2\text{O}$ is the optimum amount at which a maximum labeling of $97.3 \pm 1.87\%$ was obtained. Below this value, stannous chloride is not sufficient for complete reduction of pertechnetate to form ^{99m}Tc -complex; this is an explanation of the presence of high percentage of free pertechnetate ($39 \pm 0.31\%$ at $5 \mu\text{g}$ $\text{SnCl}_2 \cdot 2\text{H}_2\text{O}$). By increasing the amount of $\text{SnCl}_2 \cdot 2\text{H}_2\text{O}$

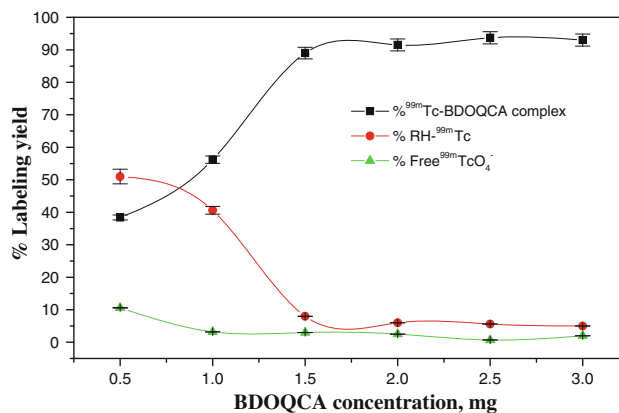


Fig. 3 Variation of the radiochemical yield of ^{99m}Tc -BDOQCA as a function of BDOQCA concentration; reaction conditions; x mg BDOQCA, $25 \mu\text{g}$ of $\text{SnCl}_2 \cdot \text{H}_2\text{O}$, 0.5 mL (~ 400 MBq) of $^{99m}\text{TcO}_4^-$ at pH 6, the reaction mixture was kept at room temperature for 30 min

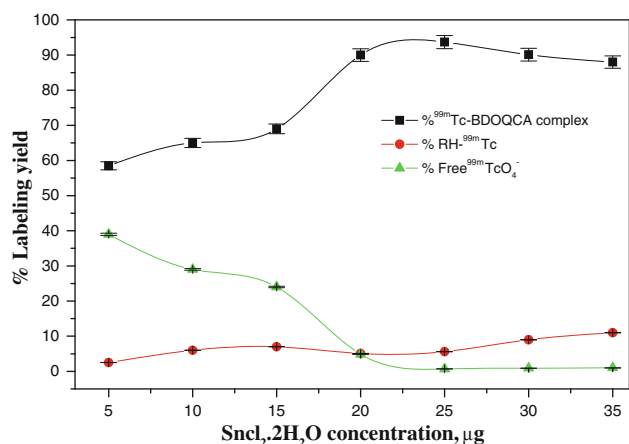


Fig. 4 Variation of the radiochemical yield of ^{99m}Tc -BDOQCA as a function of $\text{SnCl}_2 \cdot 2\text{H}_2\text{O}$ concentration; reaction conditions; 2.5 mg BDOQCA, X μg of $\text{SnCl}_2 \cdot \text{H}_2\text{O}$, 0.5 mL (~ 400 MBq) of $^{99m}\text{TcO}_4^-$ at pH 6, the reaction mixture was kept at room temperature for 30 min

above 25 μg , the radiochemical yield was decreased ($88 \pm 1.76\%$ at 35 μg $\text{SnCl}_2 \cdot 2\text{H}_2\text{O}$) while the amount of colloid increased and reach to $11 \pm 0.07\%$. This may be due to the fact that most of the ligand molecules were consumed in the formation of complexes, so the pertechnetate is reduced to insoluble technetium (IV) $\text{TcO}_2 \cdot x\text{H}_2\text{O}$ in the absence of ligand [41] or due to the fact that the excess amount of stannous chloride leads to the formation of stannous hydroxide colloid $\text{Sn}(\text{OH})_3^-$ in basic medium [42].

Effect of pH of the reaction mixture

As shown in Fig. 5 the percentage yield of ^{99m}Tc -BDOQCA increased gradually with increasing the pH up to 6 to give a labeling yield of $97.3 \pm 1.87\%$ at 30 min. At

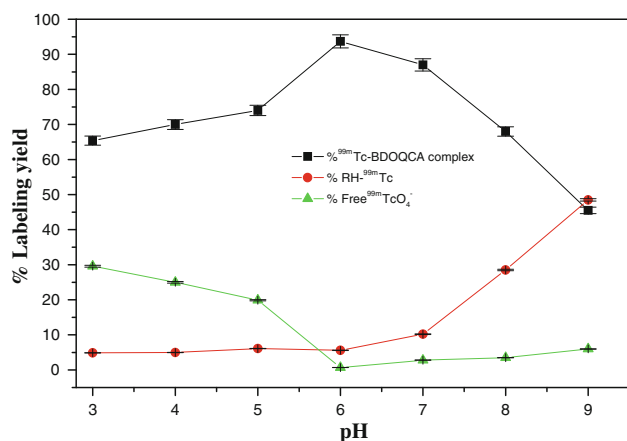


Fig. 5 Effect of pH of the reaction medium on the radiochemical yield of ^{99m}Tc -BDOQCA complex; reaction conditions; 2.5 mg BDOQCA, 25 μg of $\text{SnCl}_2 \cdot \text{H}_2\text{O}$, 0.5 mL (~ 400 MBq) of $^{99m}\text{TcO}_4^-$ at pH = X, the reaction mixture was kept at room temperature for 30 min

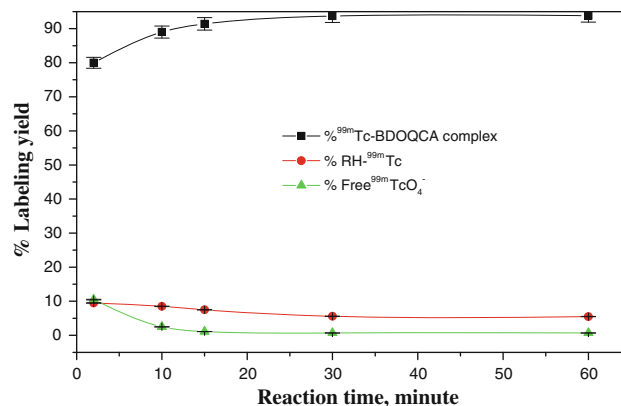


Fig. 6 Effect of the reaction time on the radiochemical yield of ^{99m}Tc -BDOQCA; reaction conditions; 2.5 mg BDOQCA, 25 μg of $\text{SnCl}_2 \cdot \text{H}_2\text{O}$, 0.5 mL (~ 400 MBq) of $^{99m}\text{TcO}_4^-$ at pH 6, the reaction mixture was kept at room temperature and at different reaction time

lower pH values, the yield was decreased till reached to $65.4 \pm 1.3\%$ at pH 3 where free pertechnetate was the main impurities. At pH above the optimum value, the radiochemical yield is drastically decreased ($45.5 \pm 0.9\%$ at pH 9) by forming $\text{RH-}^{99m}\text{Tc}$ which is the main radiochemical impurities ($48.5 \pm 0.34\%$ pH 9) where alkaline medium is a good medium for colloid formation.

Effect of reaction time and stability test:

The stability of ^{99m}Tc -complex was studied in order to determine the suitable time for injection to avoid the formation of the undesired products that result from the radiolysis of the labeled compound. These undesired radioactive products may be accumulated in non-target organs. Figure 6 shows the rate of formation of ^{99m}Tc -BDOQCA complex started relatively slowly with a yield of $80.1 \pm 1.6\%$ at 2 min reaction time. The yield was increased with time till the maximum yield of $97.3 \pm 1.87\%$ which achieved at 30 min reaction time. The formed complex was stable for a time up to 8 h.

Stability in serum

As shown in Fig. 7, incubation of the preparation containing ^{99m}Tc -BDOQCA in normal serum for 24 h at 37°C resulted in a small release of radioactivity (8.6 ± 0.6) from the ^{99m}Tc -BDOQCA, as determined by HPLC and ITLC.

In vitro binding with *E. coli*

Competition binding of the ^{99m}Tc -BDOQCA to *E. coli* was assessed by pre-incubating the bacteria with 10–100 fold excess of the unlabeled corresponding BDOQCA and then assessing the amount of radioactivity bound to the bacteria.

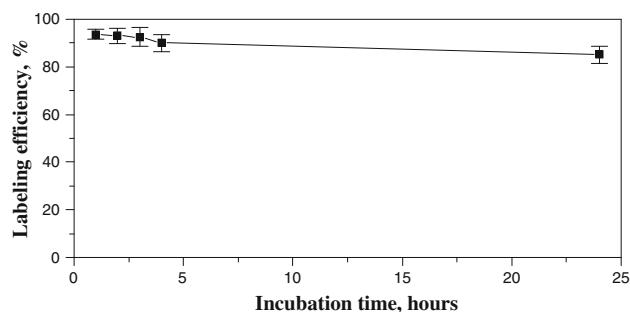


Fig. 7 Stability of ^{99m}Tc -BDOQCA in normal serum as a function of time

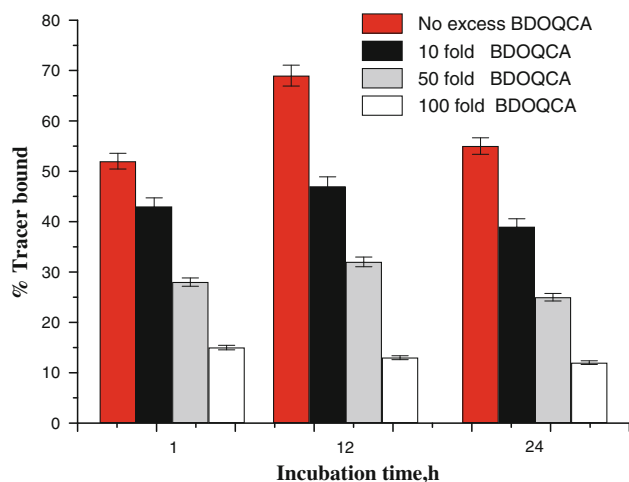


Fig. 8 In vitro binding of the ^{99m}Tc -BDOQCA to *E. coli*

Adding additional cold BDOQCA significantly decreases the binding of ^{99m}Tc -BDOQCA to living bacteria indicating that; ^{99m}Tc -BDOQCA complex is a specific agent for

bacterial cells. The in vitro binding affinity of the ^{99m}Tc -BDOQCA complexes is shown in Fig. 8.

Biodistribution

The uptake of the ^{99m}Tc -BDOQCA complex in different organs of the animals infected with living, heat killed *E. coli* and turpentine oil is given in Table 1. The uptake of ^{99m}Tc -BDOQCA was significantly low in heat killed *E. coli* and turpentine oil infected group of animals (aseptic inflammation) as compared to infected group with living bacteria (abscess). These data depicted rapid distribution throughout the body and uptake in the inflamed areas was observed within 2 h after intravenous injection of the tracer. As shown in Fig. 9, mice with infectious lesions injected with ^{99m}Tc -BDOQCA showed a mean abscess-to-muscle (target-to-non target, T/NT) ratio equal to 7.6 ± 0.6 , after 2 h post injection. ^{99m}Tc -BDOQCA shows higher T/NT in the infected muscle (live *E. coli*) at all time intervals than that of sterile inflamed muscle (heat killed

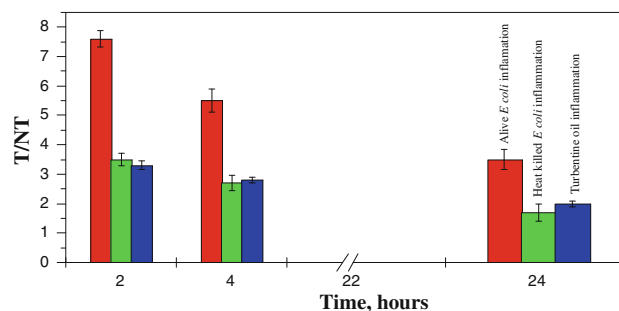


Fig. 9 The ratio of target muscle (T) to non-target muscle (NT) of ^{99m}Tc -quinoline (left) in different inflammation models at different post injection times

Table 1 Biodistribution of ^{99m}Tc -BDOQCA in *E. coli*, heat killed *E. coli* and turpentine oil inflamed mice at different time intervals

Organs and body fluids	% injected dose/organs at different time intervals (h)								
	<i>E. coli</i>			Heat killed <i>E. coli</i>			Turpentine oil		
	2	4	24	2	4	24	2	4	24
Inflamed muscle	1.9 ± 0.2	1.2 ± 0.10	0.7 ± 0.06	0.95 ± 0.1	0.71 ± 0.2	0.22 ± 0.1	1.0 ± 0.0	0.65 ± 0.2	0.24 ± 0.1
Control muscle	0.25 ± 0.1	0.22 ± 0.2	0.2 ± 0.0	0.27 ± 0.0	0.26 ± 0.1	0.13 ± 0.0	0.310 ± 0.0	0.23 ± 0.0	0.12 ± 0.0
Liver	16.1 ± 3.2	12.5 ± 2.0	5.2 ± 0.3	17.6 ± 2.4	11.2 ± 2.2	4.5 ± 0.5	16.5 ± 2.0	13.2 ± 2.1	5.1 ± 0.4
Urine	19.5 ± 3.5	26.9 ± 3.2	31.9 ± 2.1	17.1 ± 1.0	24.3 ± 1.3	30.4 ± 2.2	19.0 ± 0.9	26.4 ± 1.5	29.8 ± 2.6
Kidneys	10.2 ± 1.2	7.7 ± 0.3	4.6 ± 0.4	10.9 ± 1.3	8.2 ± 2.1	5.1 ± 0.3	11.1 ± 1.0	10.2 ± 1.2	5.9 ± 0.3
Blood	4.3 ± 0.4	3.1 ± 0.2	1.00 ± 0.0	5.10 ± 0.2	3.0 ± 0.2	1.0 ± 0.1	4.5 ± 0.2	2.3 ± 0.2	1.0 ± 0.0
Heart	0.3 ± 0.1	0.1 ± 0.0	0.09 ± 0.0	0.3 ± 0.09	0.1 ± 0.0	0.1 ± 0.0	0.4 ± 0.08	0.2 ± 0.0	0.1 ± 0.0
Lung	1.2 ± 0.2	0.2 ± 0.0	0.1 ± 0.0	1.1 ± 0.09	0.2 ± 0.0	0.1 ± 0.0	1.3 ± 0.09	0.4 ± 0.1	0.2 ± 0.0
Intestine and stomach	19.9 ± 2.5	3.90 ± 0.5	2.10 ± 0.3	19.1 ± 3.4	4.7 ± 0.4	2.2 ± 0.7	18.9 ± 1.9	4.7 ± 0.8	2.4 ± 0.4
Spleen	1.10 ± 0.1	1.00 ± 0.0	0.3 ± 0.1	1.1 ± 0.3	1.1 ± 0.0	0.4 ± 0.1	2.0 ± 0.1	1.3 ± 0.0	0.3 ± 0.0
Bone	0.70 ± 0.1	0.40 ± 0.1	0.10 ± 0.0	1.0 ± 0.0	0.35 ± 0.1	0.1 ± 0.0	1.1 ± 0.2	0.5 ± 0.1	0.1 ± 0.0

E. coli and turpentine). This ^{99m}Tc -BDOQCA showed higher uptake in infected tissue than ^{99m}Tc -ciprofloxacin ($T/NT = 3.6 \pm 0.4$). The mean abscess-to-muscle (T/NT) ratio for ^{99m}Tc -BDOQCA was higher than that of other recently published ^{99m}Tc -labeled antibiotics such as sparfloxacin ($T/NT = 5.9 \pm 0.7$) [23], difloxacin ($T/NT = 5.5 \pm 0.5$) [26], norfloxacin ($T/NT = 6.9 \pm 0.4$) [30], rifampicin ($T/NT = 7.3 \pm 0.7$) [29], ceftriaxone ($T/NT = 5.6 \pm 0.6$) [43], streptomycin ($T/NT = 2.4 \pm 0.1$) [44], and *N*-sulfanilamide ($T/NT = 2.9 \pm 0.1$) [45].

Conclusion

In this study, BDOQCA was synthesized, well characterized and labeled with ^{99m}Tc with a labeling yield of 97.3% using simple and instantaneous method. ^{99m}Tc -BDOQCA shows higher mean abscess-to-muscle (target-to-non target, T/NT) ratio in the infected muscle (live *E. coli*) at all time intervals than that of sterile inflamed muscle (heat killed *E. coli* and turpentine). ^{99m}Tc -BDOQCA complex showed higher labelling yield, stability and uptake in infected tissue ($T/NT = 7.6 \pm 0.6$) than the commercially available ^{99m}Tc -ciprofloxacin ($T/NT = 3.6 \pm 0.4$) [21]. These results were promising enough to state that ^{99m}Tc -BDOQCA could be used instead of the commercially available ^{99m}Tc -ciprofloxacin as a good radiotracer for imaging of infection at early stages and distinguishing infection from sterile inflammation.

Acknowledgments This research project was supported by a grant from the research centre of the centre for female scientific and medical colleges in King Saud University.

References

- Britton KE, Vinjamuri S, Hall AV, Solanki K, Siraj QH, Bomanji J, Das S (1997) *Eur J Nucl Med* 24:553–555
- Seabold JE, Palestro CJ, Brown ML (1997) *J Nucl Med* 38:994–997
- Staab EV, McCartney H (1978) *Semin Nucl Med* 8:219–234
- Frederick LD, David AT (1986) *J Nucl Med* 27:1849–1853
- Schrijver MD, Streule K, Senekowitsch R, Fridrich R (1987) *Nucl Med Commun* 8:895–908
- Buscombe JR, Miller RF, Luid D, Ell P (1991) *J Nucl Med Commun* 12:583–592
- McAfee JG, Gagne G, Subramanian G, Schneider RF (1991) *J Nucl Med* 32:2126–2131
- Akhtar MS, Qaisar A, Irfanullah J, Iqbal J, Khan B, Jehangir M, Nadeem MA, Khan MA, Afzal MS, Ul-Haq I, Imran MB (2005) *J Nucl Med* 46:567–573
- Akhtar MS, Iqbal J, Khan MA, Irfanullah J, Jehangir M, Khan B, Ul-Haq I, Muhammad G, Nadeem MA, Afzal MS, Imran MB (2004) *Nucl Med* 45(5):849–856
- Nibbering PH, Welling MM, Paulusma-Annemma AA, Brouwer CP, Lupetti A, Pauwels EK (2004) *J Nucl Med* 45:321–326
- Vanderlaken CJ, Boerman OC, Oyen JG, Van De Ven MT, Van De Meer JW, Corstens FH (1998) *Eur J Nucl Med* 25:535
- Pirmettis I, Limouris GS, Papadopoulos M (1999) *Eur J Nucl Med* 26:1108–1111
- Vinjamuri S, Hall AV, Solanki KK (1996) *Lancet* 347:233
- Rien HS, Huub JR, Otto CB, Rudid D, Guido S (2004) *J Nucl Med* 45:2088
- Seung JO, Jin SR, Joong WS, Eun JY, Hyun JH (2002) *J Appl Radiat Isot* 57:193
- Motaleb MA (2007) *J Radioanal Nucl Chem* 272:95–99
- Hall AV, Solanki KK, Vinjamuri S, Britton KE, Sas SS (1998) *J Clin Pathol* 51:215–219
- Sonmezoglu K, Sonmezoglu M, Halac M, Akgun I, Turkmen C, Onsel C, Kanmaz B, Solanki K, Britton KE, Uslu I (2001) *J Nucl Med* 42:567–574
- Yapar Z, Kibar M, Yapar AF, Togrul E, Kayaselcuk U (2001) *Eur J Nucl Med* 28:822–830
- Larikka MJ, Ahonen AK, Niemela O (2002) *Nucl Med Commun* 23:167–169
- Dumarey N, Blocklet D, Appelboom T, Tant L, Schoutens A (2002) *Eur J Nucl Med* 29:530–535
- Sarda L, Saleh-Mghir A, Peker C, Meulemans A, Cremieux AC, Le Guludec D (2002) *J Nucl Med* 43:239–240
- Motaleb MA (2009) *J Labelled Comp Radiopharm* 52:415–418
- El-Ghany EA, Amine AM, El-Kawy OA, Amin M (2007) *J Labelled Comp Radiopharm* 50:25–31
- El-Ghany EA, El-Kolaly MT, Amine AM, El-Sayed AS, Abdel-Gelil F (2005) *J Radioanal Nucl Chem* 266:131–135
- Motaleb MA (2010) *J Labelled Comp Radiopharm* 53:104–109
- Chattopadhyay S, Saha Das S, Chandra S, De K, Mishra M, Ranjan Sarkar B, Sinha S, Ganguly S (2010) *Appl Radiat Isot* 68:314–316
- Shah SQ, Khan AU, Khan MR (2010) *J Radioanal Nucl Chem* 284:189–193
- Shah SQ, Khan AU, Khan MR (2010) *Appl Radiat Isot* 68:2255–2260
- Ibrahim IT, Motaleb MA, Attalah KM (2010) *J Labelled Comp Radiopharm* 50:25–29
- De D, Byers LD, Krogstad DJ (1997) *J Heterocyclic Chem* 34:315–320
- Mague De D, Byers JT, Krogstad DJ (1995) *Tetrahedron Lett* 36:205–208
- Price CC, Roberts RM (1946) *J Am Chem Soc* 68:1204–1209
- Counsell RE, Pocha P, Ranade VV, Sterngold J, Beierwaltes WH (1969) *J Med Chem* 12:232–236
- De D, Krogstad FM, Byers LD, Krogstad DJ (1998) *J Med Chem* 41:4918–4926
- Welling MM, Paulusma-Annema A, Balter HS, Pauwels EKJ, Nibbering PH (2000) *Eur J Nucl Med* 27:292–297
- Laken V, Boerman CJ, Oyen OC, van de Ven WJG, Meer JWM, Corstens FHM (2000) *J Nucl Med* 41:463–469
- Oyen WJG, Boerman OC, Corstens FHM (2001) *J Microbiol Meth* 47:151–157
- Asikoglu M, Yurt F, Cagliyan O, Unak P, Ozkilib H (2000) *Appl.Rad.Isot* 53:411–413
- Rhodes BA (1974) *Semin Nucl Med* 4:281–286
- Srivastava SC, Richards P (1983) Technetium-labeled compounds. In: Rayudu GVS (ed) *Radiotracers for medical applications, CRC series in radiotracers in biology and medicine*. CRC Press, Boca Raton, pp 107–185
- Wardell JL (1994) Tin: inorganic chemistry. In: King RB (ed) *Encyclopedia of inorganic chemistry, vol 8*. Wiley, New York, pp 4159–4197
- Mostafa M, Motaleb MA, Sakr TM (2010) *Appl Rad Isot* 68:1959–1963
- Meral T, Eran T, Isil SU (1992) *J Nucl Med Biol* 19:802–806
- Imen E, Wafa G, Nadia MS, Mouldi S (2010) *J Nucl Med Biol* 37:821–829